HfO_2-based ferroelectric modulator of terahertz waves with graphene metamaterial*

Ran Jiang(蒋然)[1,†], Zheng-Ran Wu(吴正冉)[2], Zu-Yin Han(韩祖银)[3], and Hyung-Suk Jung[2]

[1] *Physical School, Shandong University, Jinan* 250100, *China*

[2] *Department of Materials Science and Engineering, Seoul National University, Seoul* 151-747, *Korea*

(Received 28 May 2016; revised manuscript received 24 June 2016; published online 25 August 2016)

Tunable modulations of terahertz waves in a graphene/ferroelectric-layer/silicon hybrid structure are demonstrated at low bias voltages. The modulation is due to the creation/elimination of an extra barrier in Si layer in response to the polarization in the ferroelectric Si:HfO_2 layer. Considering the good compatibility of HfO_2 with the Si-based semiconductor process, the highly tunable characteristics of the graphene metamaterial device under ferroelectric effect open up new avenues for graphene-based high performance integrated active photonic devices compatible with the silicon technology.

Keywords: modulation, Hafnium oxide, graphene

PACS: 68.65.Pq, 85.50.–n, 84.40.Lj **DOI:** 10.1088/1674-1056/25/10/106803

1. Introduction

Recently, manipulating terahertz electromagnetic waves has attracted extensive attention, owing to its unprecedented expectation towards the convergence of electronics and photonics, and applications in sensing, security screening, and telecommunications.[1,2] Promising functionalities of metamaterials, which possess unusual and exotic electromagnetic properties, offer an effective way to manipulate electromagnetic waves in the terahertz regime. Various metamaterial-based modulators have been well demonstrated.[3] Among them, graphene metamaterial, a two-dimensional monolayer with a planar metasurface, opens up fascinating possibilities for THz wave control. Its special Dirac cone-type electronic band structure makes the electrons behave as massless carriers, further leading to the extremely high carrier mobility,[4] which makes it an extremely attractive candidate in metamaterial design in the terahertz regime. It has been demonstrated that the terahertz waves are manipulated by using the electrical control[5] or optical illumination.[6,7] Based on these studies, here, we report a ferroelectrically controlled device to realize a tunable modulation controlling the propagation properties of the terahertz waves. The resonance response characteristics of graphene metamaterials could be dynamically tuned in this device due to the influence of ferroelectricity from the Si:HfO_2 layer.[8] The ferroelectric behavior allows the charge carrier density and the corresponding Fermi level of the graphene layer to be tuned, thus various absorbed carriers in graphene lead to distinct modulation performance,[9,10] i.e., an increase in the carrier density in graphene leads to the decrease of transmission of THz wave.[11]

In this article, a tunable modulation of the terahertz response at low voltage bias is investigated in a ferroelectric-controlled device based on a graphene metasurface. Under optical illumination, the photo-carriers generated in silicon directly diffuse into graphene by passing through an extra barrier that is induced by the ferroelectric layer, thus leading to a dynamical tuning of the Fermi level in the graphene film. The ferroelectric of the HfO_2 based layer is sensitive to the gate voltage, therefore, a small gate voltage would dramatically change the graphene conductivity and consequently modulate the terahertz response. Though there are many ferroelectric materials, their usage scope is restricted by the incompatibility of the semiconductor industrial process and the loss of the mature ultrathin fabrication method, while these requirements can be met by HfO_2 dielectric perfectly.[12–17] The ferroelectricity brought in device by the ultrathin Si:HfO_2 layer could dynamically and sensitively provide tunable modulation of THz wave with the guide of photons, which are excited by the photogenerated carriers in the semiconductor substrate, diffusing into graphene, which opens up an avenue to investigating the high performance of the integrated graphene-based devices compatible with the silicon technology.

2. Experimental details

The modulator device based on the hybrid structure is illustrated in Fig. 1. In order to allow for the transmission of the incident terahertz beam, a square metal ring was incorporated onto the surface of the devices as top and bottom electrodes, respectively. A graphene grown by copper-catalyzed chemical vapor deposition (CVD) was transferred onto the Si:HfO_2 surface: graphene was first grown on copper by the CVD, using methane and hydrogen,[18] followed by

*Project supported by the National Natural Science Foundation of China (Grant No. 11374182).

†Corresponding author. E-mail: jiangran@sdu.edu.cn

© 2016 Chinese Physical Society and IOP Publishing Ltd

a poly-(methyl methacrylate) coating. Afterwards, graphene was transferred onto the Si:HfO_2 layer by removing the copper and poly-(methyl methacrylate). The two-dimensional metasurface consisting of a 200-nm-thick aluminum cross bar was lithographically fabricated. A 4-nm-thick Si:HfO_2 layer was fabricated by using the atomic layer deposition (ALD) on a 600-μm-thick n-type silicon substrate. The atomic-scale controllability of the ALD system could place the Si dopants within the film stack by changing the ratio between the HfO_2 and SiO_2 cycles.[19] The quality of the graphene samples was characterized and verified by Raman spectroscopy. The dimension of the whole substrate was about 2 cm×2 cm, the active region was about 700 μm×700 μm, and the unit cell of the Al crossbar had a size of 120 μm×120 μm.

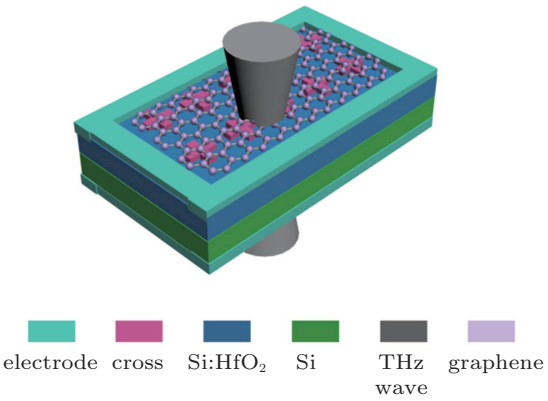


Fig. 1. (color online) Overview of the structure of ferroelectric modulator for THz wave. THz transmitted wave can be tuned by the resonant electric field of the metamaterial through enhancing the field in the vicinity of the cross bar.

A continuous wave (CW) laser of 532 nm was used to illuminate the sample. The laser power ranged from 200 mW to 400 mW. The laser beam was aligned to overlap with the THz beam with a larger light spot. The transmission spectra of the devices were characterized by the broadband terahertz time-domain spectra (THz-TDS) under different optical pump powers and bias voltages.

3. Results and discussion

The high-quality single-layer graphene can be proved by the high ratio of 2D/G and the weak D peak (located at ~1340 cm^{-1}) as shown in Fig. 2(a). The schematic diagram of the close-up view of the unit cell is shown in the inset, each unit cell of which consists of a cross bar structure and a single-layer of graphene on its top. The structural parameters of the cross bar are $W = 15$ μm and $L = 60$ μm, respectively. In this structure, the cross bar serves as a band-pass electromagnetic field concentrator, of which the center frequency (f_0) and bandwidth depend on the structure dimension of the cross bar. The resonance frequency is determined by $f_0 = 1/2\pi\sqrt{LC}$. The LC resonance line width is limited by the effective resistance (R) in the cross bar. The single-layer graphene positioned in the concentrated in-plane field region plays a role of modulating the amplitude and phase of the THz transmitted waves. At zero bias voltage, the Fermi level is at the Dirac point of the graphene, introducing minimal insertion loss, as a result, resulting in a maximal transmission of THz wave. When a bias voltage is applied, the Fermi level is tuned away from the Dirac point due to increasing intraband transition. The conductivity (σ) of the graphene layer can be described by a simple Drude model.[20] In the present work, the conductivity of the graphene changes significantly, consequently modulating the performance of THz transmitted wave sensitively.

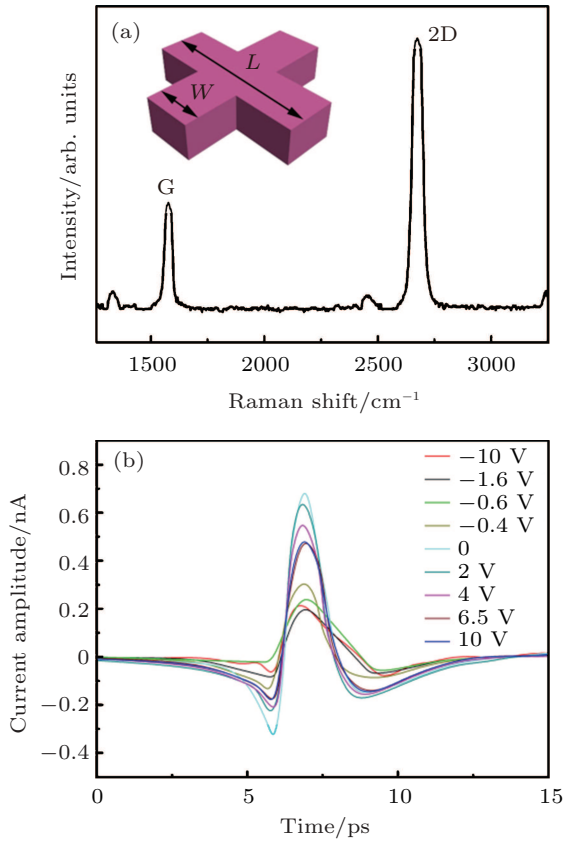


Fig. 2. (color online) Basic spectra for grapheme and modulator. (a) Raman spectrum of the graphene with the inset showing the close-up view of a unit cell with $W = 15$ μm and $L = 60$ μm. (b) Normalized terahertz time-domain signals at various gate bias voltages under a photoexcitation power of 300 mW.

The amplitude transmission is extracted from the ratio of the Fourier transformed amplitude spectrum of the sample to that of the reference one (an identical bare piece of silicon). The modulation depth is defined as

$$M_{\text{dep}} = \frac{T_{\text{g}} - T_0}{T_0},$$

where T_{g} and T_0 are the normalized time–domain transmission peaks for V_{g} and zero gate voltages, respectively. Figure 2(b) shows the measured normalized time–domain amplitudes of the device biased with different voltages under an optical illumination power $P = 300$ mW. The peak amplitude of the terahertz pulse is significantly changed with bias voltage.

In order to verify the performance of the ferroelectric modulator, figure 3(a) shows the measured amplitude transmissions with different values of applied gate bias voltage V_g under 300-mW optical excitation. A pronounced LC resonance approximately at 1.12 THz is observed. The same trends of transmission change happen when using a cross bar with different sizes or scales, in which the functioning resonance frequencies are different from each other. The voltage dependent transmission at the dip of *LC* resonance is summarized in Fig. 3(b). As the positive gate voltage increases from 0 V to 10 V, the terahertz transmission depth is enhanced, peaking at $V_g = 0$ V where the Fermi level of graphene is much closer to the Dirac point,[21] but not exactly at the Dirac point, because the graphene film examined here is prepared by use of CVD processing and is slightly p-type doped, whose Fermi energy, E_F, is near the Dirac point in the valence band. At $V_g = 10$ V, the measured amplitude modulation depth arrives at ~43% at the resonance frequency. With the further increase of V_g, however, a saturation trend of the transmission can be observed. Thus, with $V_g = 10$ V, a resonance dip as low as 0.34 is observed in the transmission spectrum. On the other hand, contrary to the gentle slope observed for the decrease of the terahertz transmission with increasing positive voltage, the transmission decreases, showing a much more drastic and steep trend under a negative voltage V_g applied. As shown in Fig. 3(b), the terahertz transmission reaches a saturation point at a relatively low voltage $V_g = -1.6$ V, where the resonance dip decreases significantly to 0.07 with a modulation depth approaching to ~89%. Figure 3(b) also shows the comparison among normalized peak values under optical illumination power $P = 200$, 300, and 400 mW, respectively. Under the illumination power $P = 200$ mW, a modulation depth of up to 34% is achieved when the bias is changed from 0 V to 10 V. With the illumination power further increasing up to 400 mW, the modulation depth goes up to a maximum value of 49% under 10-V bias applied. However, for negative voltage bias, there is no difference in modulation depth under different illumination powers, where ~89% modulation is used for all of the samples. Though the modulation depth is very high for the negative voltage, it is difficult to control this process due to the transmission being extremely sensitive to gate voltage. Additionally, the inset of Fig. 3(b) shows the *I*–*V* curve of the modulator device under the typical illumination of 300 mW. When a negative potential is applied, the current hardly changes with increasing electric field. When a positive potential is applied, the current shows nearly an exponential increase with voltage increasing. This result strongly indicates that the modulation process is related to the carrier transport through graphene.

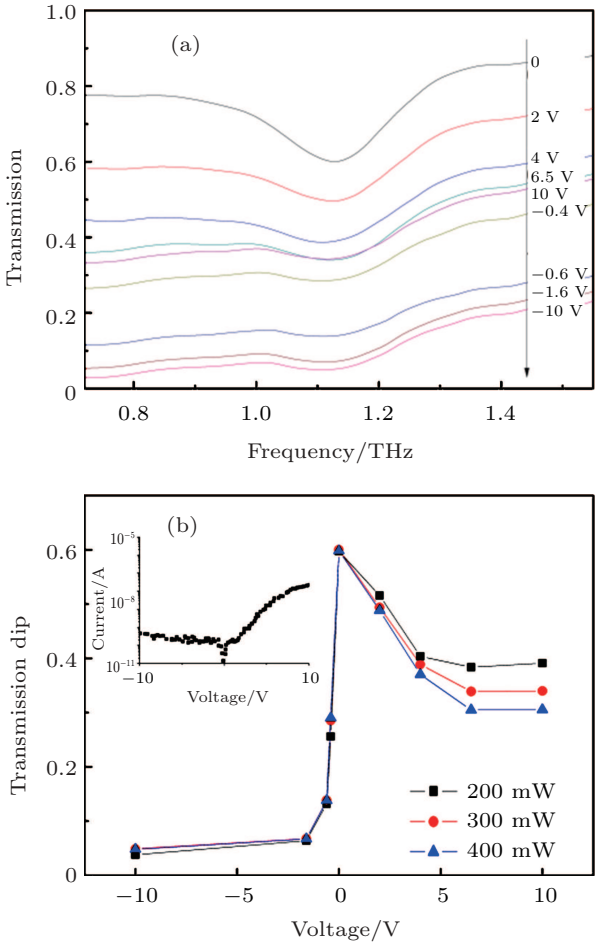


Fig. 3. (color online) Transmission and electrical behavior of the modulator. (a) Variations of transmission amplitude with frequency at various gate biases under 300-mW light illumination. (b) Gate voltage-dependent, normalized time–domain transmission peaks at the dip position of the *LC* resonance at different laser photoexcitation powers, with the inset showing the *I*–*V* curves of the device for negative and positive bias under illumination of typical 300 mW.

With varying gate voltage under optical illumination, the modulation of the transmission is attributed to the modification in the conductivity of graphene. The terahertz transmission decreases with the increase of conductivity in the graphene layer, since the larger conductivity corresponds to increased free carriers absorption at the resonance, resulting in reduced *LC* resonance strength and increased bandwidth. With continuous optical excitation, the silicon layer illuminated serves as a rich source of carriers. The free carriers diffuse from silicon into the graphene flake due to the charge gradient between their interface until an equilibrium is reached, leading to a larger gap between the Fermi level E_F and Dirac point. Figure 4 illustrates the voltage dependent transmission amplitude without any optical illumination. The absence of any significant modulation confirms the carrier diffusion from silicon into graphene.

Figure 5 illustrates the schematic diagrams of the corresponding variations of the Fermi energy E_F for various bias voltages. The terahertz transmission is ascribed to the dynamic tuning of the conductivity of the graphene film. The

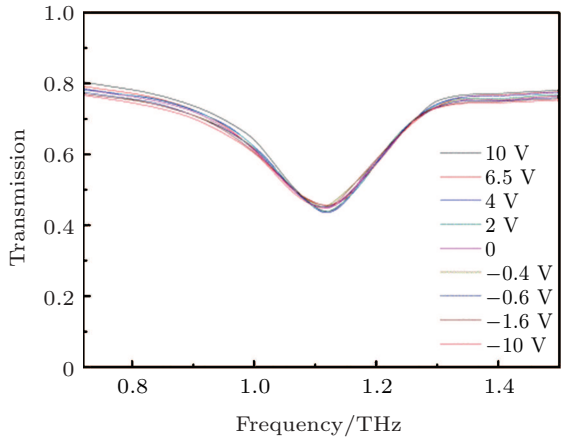


Fig. 4. (color online) Variations of measured transmission amplitude with frequency at various gate biases without illumination.

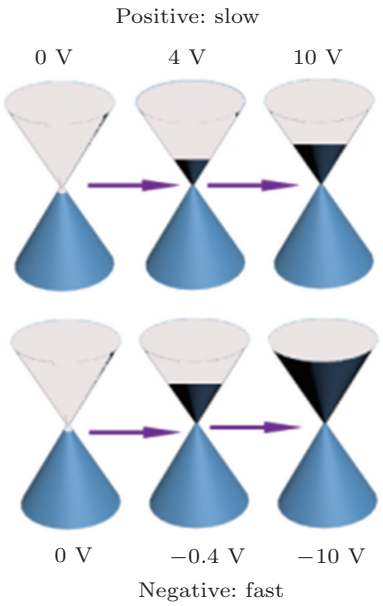


Fig. 5. (color online) Schematic diagrams of the position of Fermi energy in graphene for various bias voltages.

conductivity change causes the overall transmission modification, since E_F increases with carrier concentration increasing according to $E_F = \hbar V_F(\pi n)^{1/2}$, where V_F is the Fermi velocity, $\hbar$ is the reduced Planck constant and n is the carrier concentration. Initially, the Fermi level is near the Dirac point, while the Fermi level moves away from the Dirac point to the higher conduction band with carrier accumulation in graphene. The carrier density increasing in graphene leads to the attenuation of the terahertz transmission. At negative voltage, the Fermi level changes much more than at positive voltage as shown in Fig. 5. The electrons drift from silicon into the graphene flake. Since the graphene film examined here is prepared by the CVD and slightly p-type doped, whose Fermi energy, E_F, is near the Dirac point in the valence band, these electrons first recombine with holes in grapheme, causing the Fermi level to move toward the Dirac point. As a result, the conductivity of graphene decreases, thus enhancing the *LC* resonance of the metamaterial. The Fermi level initially moves closer to and then farther from the Dirac point in the conduction band when the positive voltage continues to increase. This strengthened the metallic property of graphene that quenches the on-resonance transmission. The above process can explain the gentle slope of tunable modulation at positive voltage. However, at negative voltage, a much lower bias voltage can very fast achieve a lower conductivity and consequently a stronger *LC* resonance than at positive voltage. This result shows that the carriers seem to be transient full-filling in graphene instead of the carriers drifting from silicon into the graphene.

To verify the working mechanism for the ferroelectric modulation of the device, the schematic drawings are shown in Fig. 6, where E_p denotes the electric field of polarization and the E_{ex} represents the external field. In the Si layer, the black dots denote the electrons. The 'circled plus' symbols in the Si layer represent positively fixed charges. The ferroelectric polarization in Si:HfO_2 points to the graphene under negative gate voltage. The positive fixed charges in the Si layer will screen the negative ferroelectric bound charges as shown in Fig. 6(a). In this case, a depleted state is determined and a space charge region spreads in the Si layer, which leads to an extra barrier in this depleted space charge region, owing to band bending induced by ferroelectric polarization as shown in Fig. 6(c). Hence, the tunneling electrons surely experience this barrier over the space charge region. Meanwhile, with the change of barrier height, there exists a width of the barrier in response to the polarization reversal, which further block the electrons from tunneling. Therefore, though almost all the applied voltage drops across the insulating interlayer (including Si:HfO_2 and depletion barrier), the growing barrier (both height and width) with increasing negative voltage can effectively block the carrier from transporting. Since at negative voltage, electron tunneling is not the main reason for the carrier accumulation in graphene, the electron injection from top metal (not

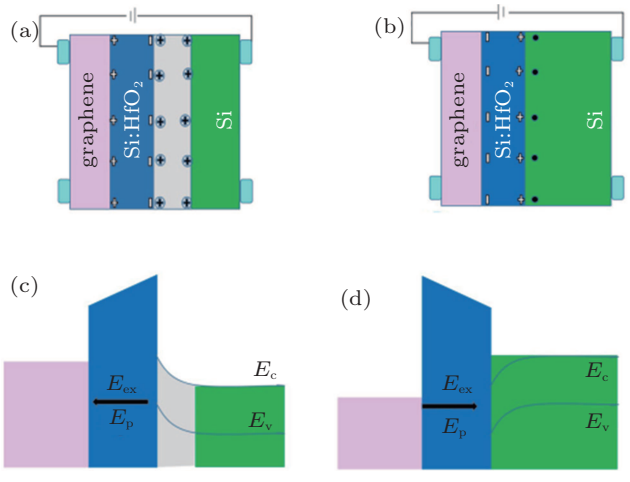


Fig. 6. (color online) Schematic drawings of the working mechanism for the modulator. Devices are under (a) negative and (b) positive bias and their potential energy profiles in panels (c) and (d), respectively.

from Si due to tunneling) into the graphene layer is supposed to be the reason why the Fermi level quickly shifts into a higher conduction band, thus further increasing the carrier density of grapheme and leading to higher attenuation of the terahertz wave.

On the other hand, when a positive voltage is applied, positive bound charges will drive the Si surface into accumulation,[22] since the polarization is reversed with the polarity bias changed into pointing to the Si. As shown in Fig. 6(b), the volume of downward domain increases with positive bias increasing, which makes the space charge region shrink to screen the increased ferroelectric bound charges. In the process of driving the polarization into pointing to the Si, the low barrier height and thin barrier width are set up. With positively increasing voltage, the electrochemical potential of graphene begins to gradually increase. Since electrons are injected into graphene by tunneling due to the external electric field and the dipole moments in the Si:HfO_2 layer. The difference in carrier density between the photoexcited semiconductor layer and graphene layers helps to result in the electrons diffusion to reach an equilibrium state.[23] The current curve increases slowly in a positive voltage region (from ~6.5 V to ~10 V). It may be highly related to the equilibrium state of the carriers between graphene and Si, meanwhile, the higher density carriers can reduce the velocity of carriers. Due to the ultrathin thickness of Si:HfO_2 and the increasing external voltage, the tunneling of electrons are kept accumulated in graphene. Therefore, the transmission decreases gradually as the bias voltage further increases until it reaches the equilibrium state. The equilibrium is highly related to the photogenerated carriers in the semiconductor layer, which is the reason why the transmission shows its dependence on the illumination power at positive voltage. Additionally, without the photoexcitation, the modulator shows a slight change with increasing the applied voltage, as shown in Fig. 4. It confirms the assumption that the diffusion of photoexcited carriers is the main reason for the carrier accumulation in graphene.

Li *et al.*[24] reported THz modulation with a diode, which shows good transmission modulation. Their report showed a similar behavior that the THz transmission is dependent on bias polarity. However, they used the diode, a fundamental electronic device that allows the current to flow just in one direction based on the polarity of the applied voltage. In the present work, the ferroelectric layer is used to adjust the modulation. The merit of the ferroelectric layer, compared with a diode, is that the modulation can be continuously tuned since the ferroelectric polarization is a dynamic response to the applied bias. A diode shows distinct state when the outer bias is switched on and off. The HfO_2 film is a well-known high-k gated dielectric in the CMOS industry. The fabrication method, including atomic layer deposition, is very mature, which assures its application in the THz device. More importantly, the HfO_2 film shows good compatibility with the process of the Si semiconductor industry, compared with other ferroelectric materials. Another merit is that a dynamic barrier is responsive to carrier modulation. This ferroelectric-induced barrier demonstrates a subtle modulation to THz wave. This barrier can be controlled well after further investigation.

4. Conclusions

In this study, a ferroelectric-based modulator is experimentally demonstrated, which behaves as an efficient tunable modulator for the terahertz waves under DC bias voltage. The structure shows distinct modulation behaviors at positive and negative voltage, due to the formation/elimination of ferroelectric induced barrier in the Si layer. Since graphene and HfO_2 are both compatible with silicon-based electronics and photonics, the active tuning behavior of the structure would enable promising applications in terahertz technology.

References

[1] Novoselov K S, Geim A K, Morozov S, Jiang D, Zhang Y, Dubonos S A, Grigorieva A and Firsov A 2004 *Science* **306** 666
[2] Bonaccorso F, Sun Z, Hasan T and Ferrari A 2010 *Nat. Photon.* **4** 611
[3] Shrekenhamer D, Rout S, Strikwerda A C, Bingham C, Averitt A D, Sonkusale S and Padilla W J 2011 *Opt. Express* **19** 9968
[4] Hashimoto A, Suenaga K, Gloter A, Urita K and Iijima S 2004 *Nature* **430** 870
[5] Chen H T, Padilla W J, Zide J M, Gossard A C, Taylor A J and Averitt R D 2006 *Nature* **444** 597
[6] Gu J, Singh R, Liu X, Zhang X, Ma Y, Zhang S, Maier S A, Tian Z, Azad A K and Chen H T 2012 *Nat. Commun.* **3** 1151
[7] Gu L L, Guo X G, Fu Z L, Wan W J, Zhang R, Tan Z Y and Cao J C 2015 *Appl. Phys. Lett.* **106** 111107
[8] Böscke T, Müller J, Bräuhaus D, Schröder U and Böttger U 2011 *Appl. Phys. Lett.* **99** 102903
[9] Xu X, Sultan S, Zhang C and Cao J 2010 *Appl. Phys. Lett.* **97** 011907
[10] Svintsov D, Otsuji T, Mitin V, Shur M and Ryzhii V 2015 *Appl. Phys. Lett.* **106** 113501
[11] Li Q, Tian Z, Zhang X, Xu N, Singh R, Gu J, Lv P, Luo L B, Zhang S and Han J 2015 *Carbon* **90** 146
[12] Jiang R, Xie E Q and Wang Z F 2006 *Appl. Phys. Lett.* **89** 142907
[13] Jiang R and Li Z 2008 *Appl. Phys. Lett.* **92** 2919
[14] Dong H, Brennan B, Zhernokletov D, Kim J, Hinkle C and Wallace R 2013 *Appl. Phys. Lett.* **102** 171602
[15] Jiang R, Du X, Han Z and Sun W 2015 *Appl. Phys. Lett.* **106** 173509
[16] Jiang R, Wu Z, Du X, Han Z and Sun W 2015 *Appl. Phys. Lett.* **107** 013502
[17] Jiang R, Wu Z, Du X, Han Z and Sun W 2015 *Appl. Phys. Lett.* **106** 252902
[18] Li X, Cai W, An J, Kim S, Nah J, Yang D, Piner R, Velamakanni A, Jung I and Tutuc E 2009 *Science* **324** 1312
[19] Lomenzo P D, Takmeel Q, Zhou C, Liu Y, Fancher C M, Jones J L, Moghaddam S and Nishida T 2014 *Appl. Phys. Lett.* **105** 072906
[20] Sensale-Rodriguez B, Yan R, Kelly M M, Fang T, Tahy K, Hwang W S, Jena D, Liu L and Xing H G 2012 *Nat. Commun.* **3** 780
[21] Ren L, Zhang Q, Yao J, Sun Z, Kaneko R, Yan Z, Nanot S, Jin Z, Kawayama I and Tonouchi M 2012 *Nano Lett.* **12** 3711
[22] Mathews S, Ramesh R, Venkatesan T and Benedetto J 1997 *Science* **276** 238
[23] Weis P, Garcia-Pomar J L, Höh M, Reinhard B, Brodyanski A and Rahm M 2012 *ACS Nano* **6** 9118
[24] Li Q, Tian Z, Zhang X Q, Singh R, Du L L, Gu J Q, Han J G and W L Zhang 2015 *Nat. Commun.* **6** 7082